

Transient electronic anisotropy in overdoped $\text{NaFe}_{1-x}\text{Co}_x\text{As}$ superconductorsShenghua Liu,¹ Chunfeng Zhang,^{1,2,*} Qiang Deng,¹ Hai-hu Wen,¹ Jian-xin Li,¹ Elbert E. M. Chia,³
Xiaoyong Wang,¹ and Min Xiao^{1,2,4,†}¹*National Laboratory of Solid State Microstructures, School of Physics, and Collaborative Innovation Center of Advanced Microstructures, Nanjing University, Nanjing 210093, China*²*Synergetic Innovation Center in Quantum Information and Quantum Physics, University of Science and Technology of China, Hefei, Anhui 230026, China*³*Division of Physics and Applied Physics, School of Physical and Mathematical Sciences, Nanyang Technological University, Singapore 637371, Singapore*⁴*Department of Physics, University of Arkansas, Fayetteville, Arkansas 72701, USA*

(Received 11 July 2017; published 19 January 2018)

By combining polarized pump-probe spectroscopic and Laue x-ray diffraction measurements, we have observed nonequivalent transient optical responses with the probe beam polarized along the x and y axes in overdoped $\text{NaFe}_{1-x}\text{Co}_x\text{As}$ superconductors. Such transient anisotropic behavior has been uncovered in the tetragonal phase with the doping level and temperature range far from the borders of static nematic phases. The measured transient anisotropy can be well explained as a result of nematic fluctuation driven by an orbital order with energy splitting of the d_{xz} - and d_{yz} -dominant bands. In addition, the doping level dependence and the pressure effect of the crossover temperature show significant differences between the transient nematic fluctuation and static nematic phase, implying spin and orbital orders may play different roles in static and transient nematic behaviors.

DOI: [10.1103/PhysRevB.97.020505](https://doi.org/10.1103/PhysRevB.97.020505)

Understanding the origin of electronic nematicity has been a central challenge in the study of iron-based superconductors (FeSCs). It is suggested that the electronic interaction underlying the nematic phase may intrinsically give rise to the formation of Cooper pairs [1–4]. Electronic nematicity at the normal state is manifested as the rotation symmetry breaking with strong anisotropy in an electronic response [4–26]. In electron-doped pnictides, evidence of nematic phases has been captured by characterizing various properties with different experimental approaches [3,4,13,14,17,25–30]. In theory, models have been proposed to explain the electronic nematicity by considering magnetic [23,26,31–34] or orbital orders [15,20,25,28,35–37]. Nevertheless, the transitions of nematic phases observed in underdoped FeSCs largely occur at the borders of magnetic and structural phase transitions [7,13,25,26,38], making it highly controversial to assign an exact origin to the observed nematic behaviors. Here, we report the observation of anisotropic transient optical responses with polarized pump-probe spectroscopy in the tetragonal phase of overdoped $\text{NaFe}_{1-x}\text{Co}_x\text{As}$ superconductors. Transient anisotropic behavior has been found in the temperature and doping range far from the borders of the static nematic phase. The results can be explained by the nematic fluctuation of the orbital order with energy splitting of the d_{xz} - and d_{yz} -dominant bands [18,28], suggesting an important role played by the orbital order in the electronic nematicity in FeSCs.

The most intuitive evidence of nematic phases is perhaps the in-plane resistivity anisotropy measured in several families of

FeSCs when a uniaxial pressure is applied to detwin the crystals [3,7,11,38]. Such in-plane anisotropy has been characterized by many other techniques including scanning tunneling spectroscopy (STM) [4,14,17], torque measurements [12], angle-resolved photoemission spectroscopy (ARPES) [28,39–41], neutron scattering [23,26,42], nuclear magnetic resonance (NMR) [22,25], and optical spectroscopy [30]. Many experiments suggest the proximity between the nematic phase and the magnetic order [4,19,23,26,31,43], however, ARPES measurements have observed clear features of ferro-orbital ordering at the Fermi surface [28,39]. The involvement of different degrees of freedom, which may be coupled to each other, makes it highly controversial to pin down the underlying mechanism. Ultrafast pump-probe spectroscopy is potentially a powerful tool to study this issue. The time-resolved capability enables us to study the dynamics of the fluctuation order parameters. By monitoring the nonequilibrium dynamics of photoexcited quasiparticles, different order parameters and their interrelations can be disentangled in the temporal domain [44–55]. To first-order approximation, the variations in spin/orbital order can be distinguished with circularly/linearly polarized probe light [19,56,57]. For example, in the system of Co-doped BaFe_2As_2 superconductors, the nematic behaviors due to spin order and orbital order have been characterized by changes in probe ellipticity [19] and polarization [56], respectively.

Here, we employ polarized pump-probe spectroscopy to investigate the dynamics of nematic fluctuations in $\text{NaFe}_{1-x}\text{Co}_x\text{As}$ superconductors with an emphasis on the rarely explored overdoped range. Samples of $\text{NaFe}_{1-x}\text{Co}_x\text{As}$ (with Co doping x from 0% to ~5%) single crystals were grown by the flux method using NaAs as the flux, as previously

*cfzhang@nju.edu.cn

†mxiao@uark.edu

reported [38,58]. The crystals were cleaved with fresh surfaces and mounted on a cold finger within an optical cryostat (MicroCryostatHe, Oxford) for temperature-dependent measurements. A Ti:sapphire mode locking laser (80-MHz repetition rate, Vitora, Coherent, Inc.) was used to perform collinear pump-probe spectroscopy with a two-color configuration: the probe wavelength at 800 nm and the pump wavelength (its second harmonic) at 400 nm. The penetration depths of the pump and probe beams were estimated to be ~ 25 and ~ 35 nm, respectively [59]. The transient reflectivity change as a function of pump-probe time delay (t) [i.e., $\Delta R/R(t)$] was detected by an avalanche photodiode and analyzed with a lock-in amplifier when the pump beam was modulated at 1 MHz by an electro-optical modulator. The diameters of pump and probe were ~ 13 and ~ 4 μm , respectively. The data presented in this Rapid Communication were captured under a weak pump fluence condition (< 1 $\mu\text{J}/\text{cm}^2$) unless otherwise specified, which is far below the saturation fluence in the linear regime (see the Supplemental Material [60] for details). The temperature rise of the illuminated spot has been accounted for in all the data. We recorded the data in the temperature range of 8–120 K. Bandpass filters were employed to exclude the scattered pump light. By using this configuration, the signal-to-noise ratio in $\Delta R/R$ reaches $\sim 10^{-6}$. To connect probe light polarization with the crystal axes, we performed Laue x-ray diffraction experiments on the crystals with and without applying uniaxial pressure.

The lattice structure of $\text{NaFe}_{1-x}\text{Co}_x\text{As}$ superconductors is dependent on the doping level x . For $x < 0.025$, the transition from an orthorhombic to tetragonal phase occurs at temperature T_S [61]. Above T_S or at a higher doping level, the samples of $\text{NaFe}_{1-x}\text{Co}_x\text{As}$ superconductors have a tetragonal lattice structure with equivalent x, y directions, as schematically shown in Fig. 1(a). We first perform measurements on an overdoped sample with $x \approx 0.05$ having the transition temperature (T_c) of the superconducting phase at ~ 16 K. During static measurements, the static reflectivity of probe light is independent of the probe polarization (see Supplemental Material, Fig. S1 [60]). We record the time-dependent $\Delta R/R(t)$ by changing polarizations of the pump and probe beams in the xy plane. The signal of $\Delta R/R$ is strongly dependent on the probe polarization [Figs. 1(b) and 1(c)], but is largely independent of the pump polarization (see Supplemental Material, Fig. S1 [60]), indicating that the probe polarization dependence is an intrinsic effect rather than a consequence of polarized pumping. We connect the anisotropic polarization dependence to the lattice structure with Laue x-ray diffraction, as shown in Fig. S2 [60]. The maximum negative signal of the long component (at a time delay of 10 ps) at 8 K has been found when the probe polarization is aligned obliquely in the middle of two axes of the tetragonal lattice. Such a correlation has been confirmed in all samples with different doping levels. We have further checked the alignment in the parent NaFeAs sample with and without applying a uniaxial pressure. A maximum negative signal is observed when the probe is polarized along the b_o axis of the orthorhombic phase (Fig. S2 [60]). We then tentatively assign the probe polarization with a maximum value of the negative long-lived component aligned to the b_o axis (i.e., 45° with respect to the a_T axis of the tetragonal lattice). Hereafter, the angle of the probe

polarization is labeled θ with respect to the direction of the maximum negative signal.

The θ dependence of the transient differential signal is quantitatively analyzed by a phenomenological model with two exponential decay components defined by

$$\Delta R/R(t) = A_1 e^{-t/\tau_1} + A_2 e^{-t/\tau_2} + A_3. \quad (1)$$

Here, $A_1(A_2)$ and $\tau_1(\tau_2)$ are the fitting parameters of the amplitude and lifetime of the fast (slow) component, respectively; A_3 is a constant representing a decay component with a lifetime much longer than the concerned time window. Despite their strong dependences on the probe polarization, the traces of transient reflectivity probed at different polarizations can be well reproduced with the same pair of lifetime parameters for a given temperature ($\tau_1 \sim 1.5$ ps and $\tau_2 \sim 124$ ps at 8 K; $\tau_1 \sim 2.5$ ps and $\tau_2 \sim 105$ ps at 26 K). It was proposed that the two decay components with different lifetime parameters may be relevant to the intraband and interband processes [62], respectively. The amplitudes (A_1 and A_2) show twofold symmetric (C_2) dependences on θ , breaking the fourfold symmetry (C_4) of the tetragonal phase. The pump-probe signal can be analyzed as a third-order nonlinear optical response [63], which is equivalent to the Raman-like description in cuprates [64] (see Supplemental Material for details [60]).

The anisotropic response is strongly dependent on temperature (T). The pump-probe traces recorded with $\theta = 0^\circ$ and 90° at different temperatures are compared in Fig. 2(a). To highlight the anisotropic part, we subtract the signal recorded with $\theta = 90^\circ$ from that recorded with $\theta = 0^\circ$ [i.e., $\Delta R/R_{\text{ani}} = \Delta R/R(0^\circ) - \Delta R/R(90^\circ)$] to eliminate the isotropic electronic and thermal responses of conventional metallic phases. The rescaled data are plotted as a function of delay time and temperature in Fig. 2(b). With increasing temperature, a peak in $\Delta R/R_{\text{ani}}$ is observed at T_c and the anisotropy disappears above T^* [Fig. 2(c)]. In the superconducting phase ($T < T_c$), the anisotropic part consists of a long-lived negative component following an ultrafast relaxation process from the positive part. The signal at the superconducting phase persists to a much longer time scale up to ~ 1 ns (Fig. S3 [60]). An additional slow component with a lifetime of ~ 830 ps is necessary to reproduce the full scale kinetics, which is likely to be a result of the phonon bottleneck effect during pair reformation in superconductors [45,46,51]. Apparently, the biexponential decay function [Eq. (1)] is sufficient to reproduce the full kinetics above T_c as the superconducting gap is absent in this temperature range (Fig. S3 [60]). Figures 2(d) and 2(e) plot the fitted amplitudes and lifetime parameters of the two decay components versus temperature at the normal state. Their amplitudes decrease gradually with increasing temperature from T_c to T^* . The lifetime of the slow decay component remains largely in the range of 100–150 ps, while the lifetime of the fast decay component decreases from ~ 3 to < 1 ps approximately following a near $1/T$ dependence in the normal state [Fig. 2(d)].

The anisotropic characteristics in pump-probe traces have been observed in all the samples from the parent phase to the overdoped range (see Fig. 3, and Figs. S4, S7, and S8 in the Supplemental Material [60]). The dependence of the crossover temperature (T^*) on the doping level is compared

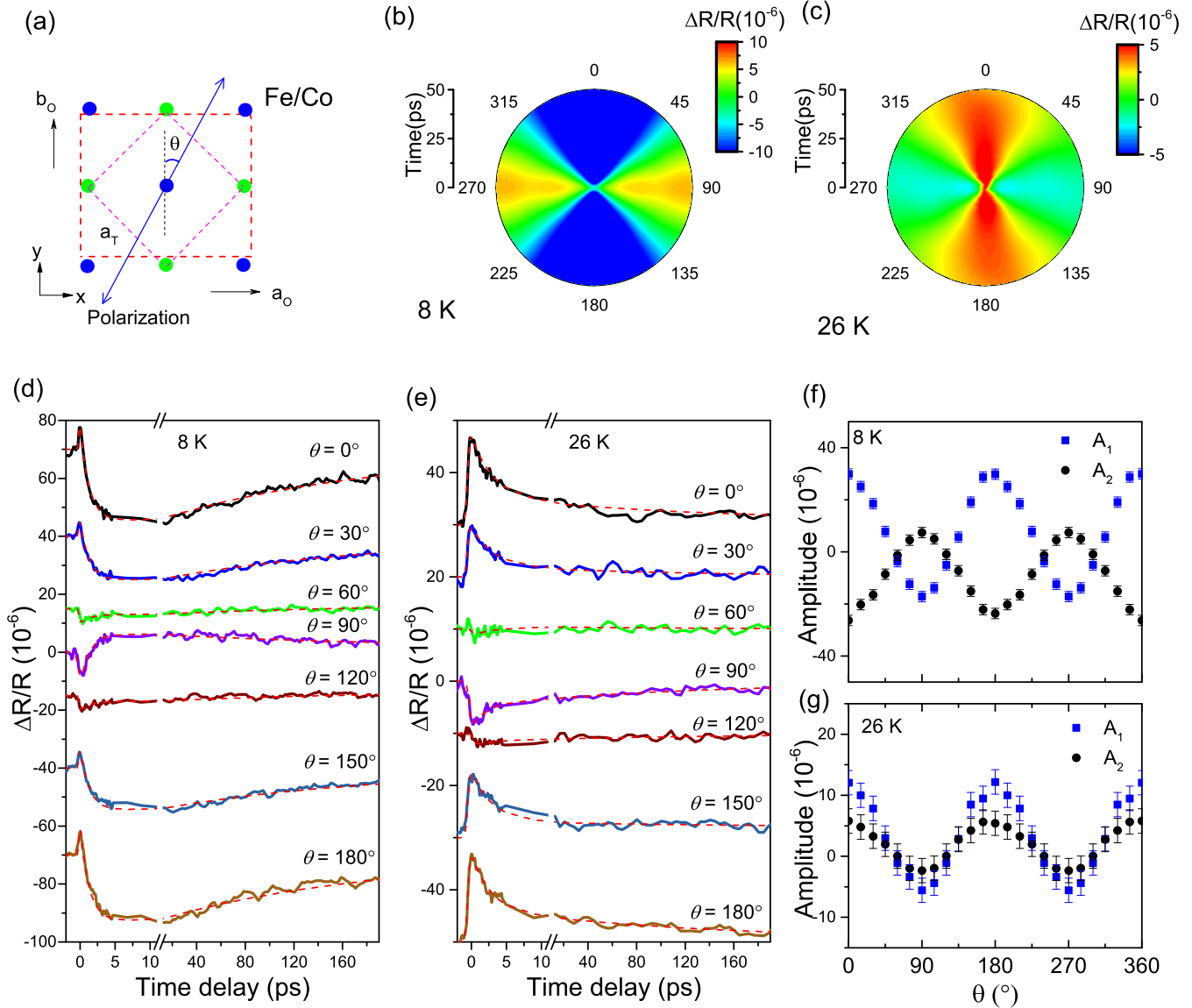


FIG. 1. Polarization-dependent differential reflectivity $\Delta R/R(t)$ recorded from $\text{NaFe}_{1-x}\text{Co}_x\text{As}$ ($x \approx 0.05$, $T_c \approx 16$ K). (a) Schematic diagram of the probe polarization with respect to the in-plane lattice axes. The square and rectangle represent the tetragonal and orthorhombic lattice, respectively. Different colors indicate the Fe/Co atoms at different planes. (b), (c) Polar plot of polarization dependence of $\Delta R/R(t)$ recorded at 8 and 26 K, respectively. (d), (e) Time-resolved traces of $\Delta R/R(t)$ recorded with different probe polarizations at 8 and 26 K, respectively. (f), (g) Polarization-dependent amplitudes of fast and slow components of data (d), (e) fitted to a biexponential decay component, respectively.

with the crossover temperature of nematic states measured by transport (T_{nem}) as well as the transition temperatures of lattice structures (T_S), spin-density-wave (SDW) orders (T_M), and the superconducting phase (T_c) (Fig. 4). The anisotropic transient optical responses reveal the nematic electronic behaviors in the tetragonal phase, which appear in the temperature and doping range far from the borders of the structural and magnetic transitions. Importantly, the nematic phase has not been studied under those conditions by any static measurements. The transient anisotropic response can be induced by a nematic fluctuation. In theory, a nematic fluctuation in the tetragonal phase can be modeled with the scenario of magnetic [32] or orbital [65] orders. The transient anisotropic behavior observed under weak perturbation is not directly relevant to the

fluctuated magnetic order, since a change in the ellipticity of the probe light has not been observed. Alternatively, an orbital scenario with energy splitting of $3d_{xz}$ and $3d_{yz}$ orbitals can qualitatively explain the major findings [28,66,67]. The optical response at 1.55 eV in ferropnictides is primarily contributed by the transitions of Fe-3d electrons [68,69]. Near the Fermi surface, the orbitals of d_{xz} , d_{xy} , and d_{yz} dominate the density of states. The polarization-dependent electronic transitions are orbital selective ones. When the light is polarized along x , the nonzero transitions are $d_{xz} \leftrightarrow d_{x^2-y^2}/d_{z^2}$, $d_{yz} \leftrightarrow d_{xy}$, and $d_{xy} \leftrightarrow d_{yz}$; when the light is polarized along y , the nonzero transitions are $d_{xz} \leftrightarrow d_{xy}$, $d_{yz} \leftrightarrow d_{x^2-y^2}/d_{z^2}$, and $d_{xy} \leftrightarrow d_{xz}$ (Fig. S6 [60]) [70]. With no nematic order, optical signals with the probe beam polarized at the x and y axes are equivalent.

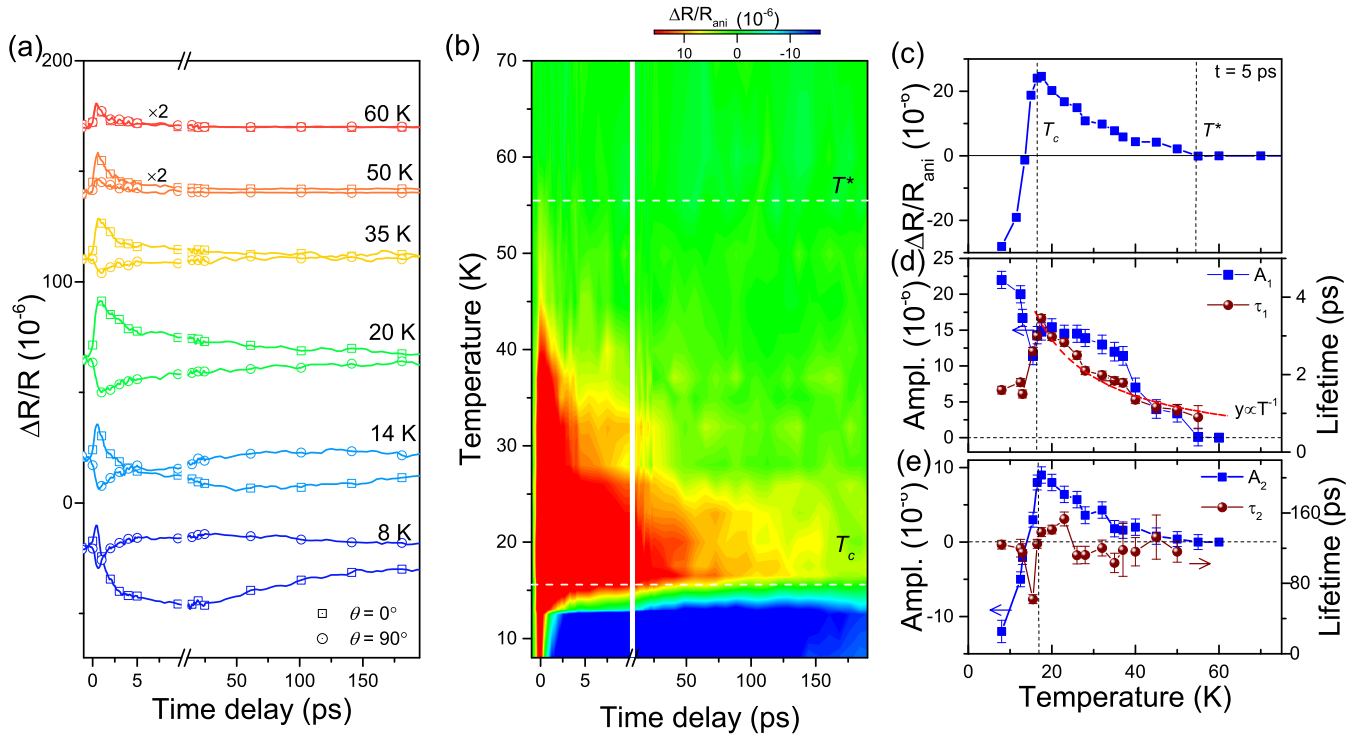


FIG. 2. Temperature dependence of anisotropic response in $\text{NaFe}_{1-x}\text{Co}_x\text{As}$ ($x \approx 0.05$). (a) Time-resolved kinetics of differential reflectivity probed with polarization angles $\theta = 0^\circ$ and $\theta = 90^\circ$ at different temperatures, respectively. (b) The anisotropic part [$\Delta R/R_{\text{ani}} = \Delta R/R(0^\circ) - \Delta R/R(90^\circ)$] is plotted as a function of time delay and temperature. (c) The signal difference at a time delay of 5 ps is plotted vs temperature. (d) Temperature-dependent amplitudes and (e) lifetime parameters of the fast and slow components of data (b) fitted to the biexponential decay function, respectively.

When the nematic fluctuation is driven by orbital order, the energy splitting of d_{xz} and d_{yz} near the Fermi surface causes a different population in the two orbitals. In consequence, the optical response is nonequivalent with the probe polarized along the x or y axis [Fig. 3(g)], leading to the observed results in this work. Nevertheless, the formation of twin domains with different orthogonal possibilities may average out the anisotropic response of a nematic phase. In static transport measurements, an external pressure is applied to detwin the structure for capturing the anisotropic response. For transient optical measurements, the exact mechanism for structural detwinning is yet to be illustrated. It has been proposed that the surface strain due to a laser-induced crystal expansion may help to detwin the dynamic nematicity [56], which may explain why a nematic fluctuation can be observed here.

In the literature, the approximation of single-particle excitation has been widely adopted to interpret pump-probe data recorded from high-temperature superconductors [44]. In this scheme, the recovery lifetime at the normal state is determined by the gap energy of the order parameter [46,56,71]. In overdoped $\text{NaFe}_{1-x}\text{Co}_x\text{As}$, STM measurements have captured the feature of a temperature-independent gap above T_c [72]. The decay lifetime should be independent of temperature in the scheme of single-particle excitation, which, however, conflicts with the strong temperature dependence of the decay lifetime observed here [Fig. 2(d)]. Apparently, the impulsive excitation of quasiparticles coupled to a collective degree of freedom may be an alternative picture, which was proposed to explain the normal state dynamics in electron-doped cuprates [50].

The dynamics of the transient nematic behavior observed in this work can be better understood within such a scenario of impulsive excitation. Two possible processes may be involved: (1) The nematic fluctuation is triggered by a direct coupling between the quasiparticles and the orbital order. In this case, the orbital order fluctuation is triggered simultaneously with photoexcited quasiparticles. (2) The nematic fluctuation is related to an orbital order by the coupling between the quasiparticles and the local strain through the Raman interaction [50]. In this case, the local crystal expansion induced by pulse excitation drives the instability of the tetragonal lattice dynamically, which further causes a fluctuation of orbital order. The doping-dependent behavior of T^* observed here shows some similarity with a previous analysis on the retention of the structural transition in the $\text{SmFeAs}(\text{O}_{1-x}\text{F}_x)$ system [73], which is also relevant to the orbital order. Another possible cause of the anisotropic response is a nematicity order hidden in the isotropic phase. The anisotropic signal becomes detectable when the isotropic order is destroyed under an optical pump. Nevertheless, such a scenario is unlikely to be the major mechanism here. If the anisotropy is induced by destroying an isotropic order, the anisotropic response may become more distinct with increasing pump power, which is conflicting with the results of fluence-dependent experiments. The anisotropic response is also present under a very weak pump (Fig. S5 [60]), and the amplitude ratio of the anisotropic part is not sensitive to the pump power. Alternatively, it is possible that a slight anisotropy exists in the ground state which is too weak to be probed by static measurements. The

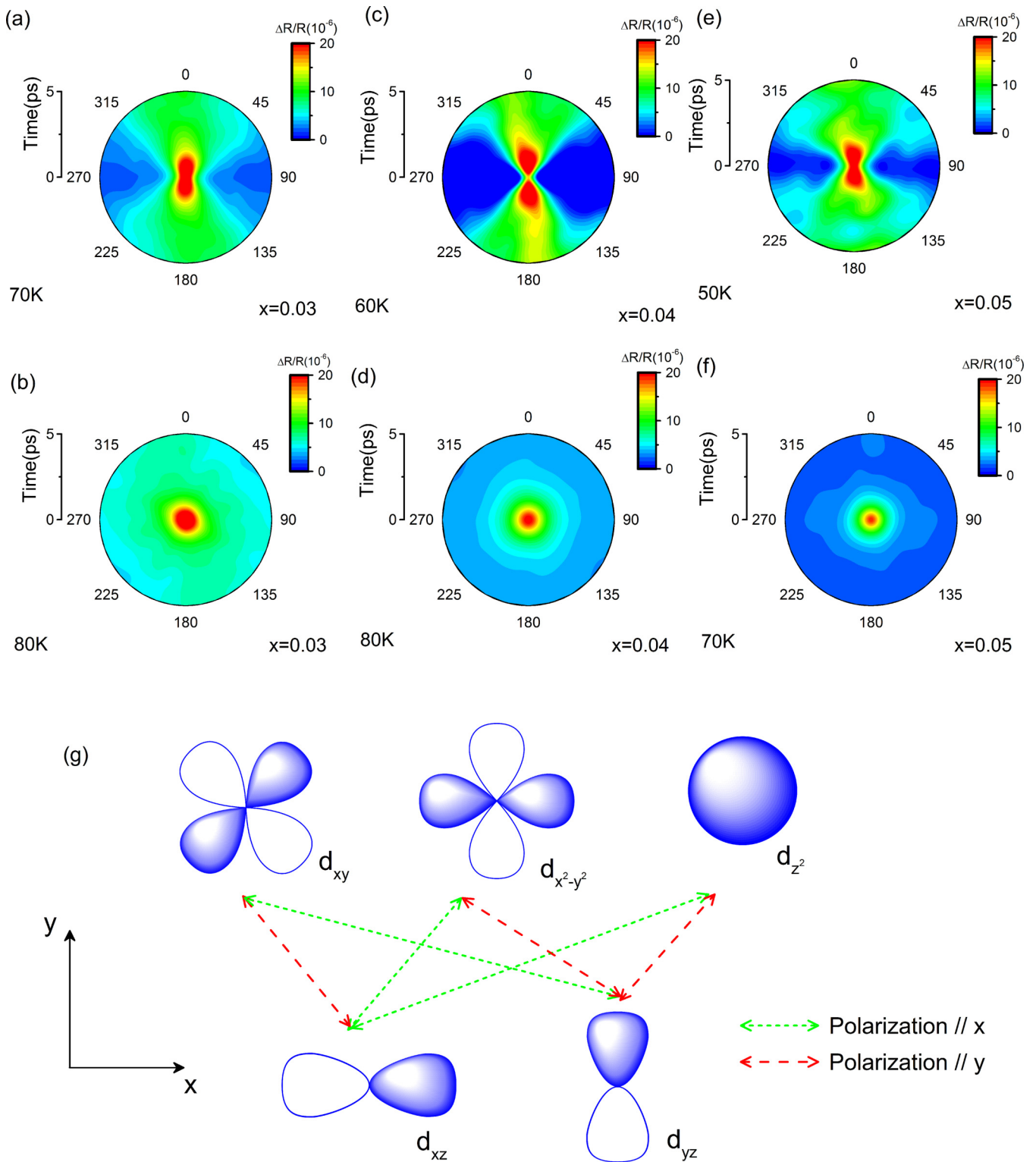


FIG. 3. Polarization-dependent transient reflectivity of $\text{NaFe}_{1-x}\text{Co}_x\text{As}$ samples with different dopings [(a), (b) $x \approx 0.03$, (c), (d) 0.04, and (e), (f) 0.05] recorded below and above the transition temperature from anisotropic to isotropic phases. (g) A diagram showing the possible mechanism responsible for the transient anisotropic response. The electric dipole-allowed transitions involving specific orbitals are schematically shown when the probe is polarized along the x and y axes, respectively (see text).

optical pump drives the system to a fully isotropic state so that the signal of differential reflectivity displays anisotropy. A further in-depth study is necessary to confirm or exclude the possibility.

Previous static measurements have shown a monotonic decrease of the transition temperature (T_{nem}) of the static nematic phase with increasing doping level from zero to optimal doping (Fig. 4) [17,25,38]. In contrast, the crossover

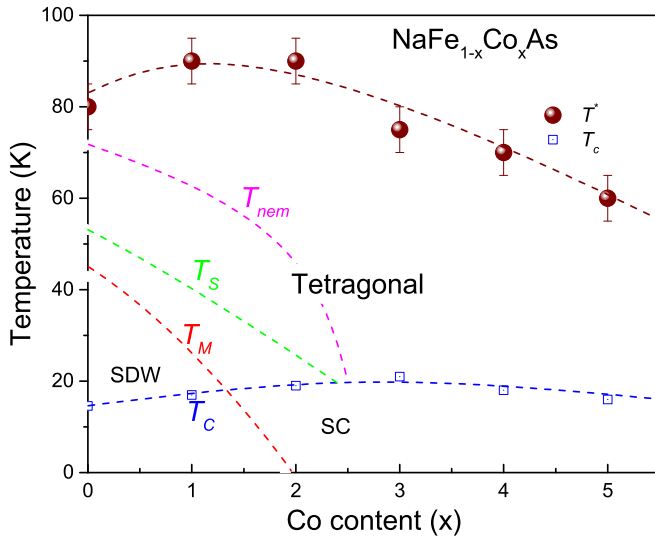


FIG. 4. Doping-level-dependent crossover temperature (T^*) of the transient nematic response in $\text{NaFe}_{1-x}\text{Co}_x\text{As}$ is shown in the phase diagram obtained by static measurements (SDW: spin-density-wave phase; SC: superconducting phase). T_c , T_M , T_S , and T_{nem} are literature values of the transition temperatures for superconductivity [38], SDW [61,79], structure transition [61], and nematic phases [38] obtained by transport measurements. The superconducting transition temperatures of the samples obtained from this work are also included.

temperature (T^*) of the transient nematic fluctuation shows a nonmonotonic dependence on the doping level, which implies the possibility of different origins underlying the nematic behavior identified by static and transient approaches. Such a divergence is also revealed with different pressure effects on the static and transient nematic behaviors in the parent sample of NaFeAs . For static transport measurements, the resistivity anisotropy is manifested only by applying a uniaxial pressure to detwin the samples. However, the pressure suppresses the

transient anisotropic response with a significant drop in the transition temperature (T^*) (Fig. S4 [60]). It is possible that the fluctuation in orbital order induces transient nematic behavior but other degrees of freedom play a more important role in the static nematic phase. In addition, anisotropy in the transient electronic response has been found in the superconducting phase, suggesting the coexistence of superconductivity and nematic order. The anticorrelation between them can be established by analyzing the fluence dependences of the characteristic signals (Fig. S5 [60]) [74].

To conclude, we have observed a transient nematic fluctuation manifested by strong anisotropic responses of the differential reflectivity in $\text{NaFe}_{1-x}\text{Co}_x\text{As}$ superconductors. Transient nematic behavior has been found in samples covering a broad range of temperature and doping levels, far exceeding the borders of the nematic phases characterized by static measurements. Such anisotropic responses are explained as a consequence of the fluctuation of orbital order with the energy splitting of the d_{xz} - and d_{yz} -dominant bands. The transient nematic behaviors show significant differences from the static nematic phase in terms of doping level dependence and pressure effect, implying an important role played by the orbital order in the nematic behaviors in FeSCs. The findings in FeSCs may also stimulate interests in investigating the mechanisms of exotic manifestations of nematic order in cuprates [6,8,9,75] and other strongly correlated materials [5,76–78] by probing polarization-dependent charge dynamics with ultrafast pump-probe spectroscopy.

This work is supported by the National Key R&D Program of China (2017YFA0303703 and 2013CB932903), the National Natural Science Foundation of China (11574140 and 11621091), Jiangsu Provincial Funds for Distinguished Young Scientists (BK20160019), the Priority Academic Program Development of Jiangsu Higher Education Institutions (PAPD), and the Fundamental Research Funds for the Central University. The authors acknowledge Dr. Xuewei Wu for his technical assistance.

- [1] E. Fradkin, S. A. Kivelson, M. J. Lawler, J. P. Eisenstein, and A. P. Mackenzie, *Annu. Rev. Condens. Matter Phys.* **1**, 153 (2010).
- [2] S. Lederer, Y. Schattner, E. Berg, and S. A. Kivelson, *Phys. Rev. Lett.* **114**, 097001 (2015).
- [3] H.-H. Kuo, J.-H. Chu, J. C. Palmstrom, S. A. Kivelson, and I. R. Fisher, *Science* **352**, 958 (2016).
- [4] E. P. Rosenthal, E. F. Andrade, C. J. Arguello, R. M. Fernandes, L. Y. Xing, X. C. Wang, C. Q. Jin, A. J. Millis, and A. N. Pasupathy, *Nat. Phys.* **10**, 225 (2014).
- [5] R. A. Borzi, S. A. Grigera, J. Farrell, R. S. Perry, S. J. S. Lister, S. L. Lee, D. A. Tennant, Y. Maeno, and A. P. Mackenzie, *Science* **315**, 214 (2007).
- [6] V. Hinkov, D. Haug, B. Fauque, P. Bourges, Y. Sidis, A. Ivanov, C. Bernhard, C. T. Lin, and B. Keimer, *Science* **319**, 597 (2008).
- [7] J.-H. Chu, J. G. Analytis, K. De Greve, P. L. McMahon, Z. Islam, Y. Yamamoto, and I. R. Fisher, *Science* **329**, 824 (2010).
- [8] R. Daou, J. Chang, D. LeBoeuf, O. Cyr-Choiniere, F. Laliberte, N. Doiron-Leyraud, B. J. Ramshaw, R. Liang, D. A. Bonn, W. N. Hardy, and L. Taillefer, *Nature (London)* **463**, 519 (2010).
- [9] M. J. Lawler, K. Fujita, J. Lee, A. R. Schmidt, Y. Kohsaka, C. K. Kim, H. Eisaki, S. Uchida, J. C. Davis, J. P. Sethna, and E.-A. Kim, *Nature (London)* **466**, 347 (2010).
- [10] R. M. Fernandes, E. Abrahams, and J. Schmalian, *Phys. Rev. Lett.* **107**, 217002 (2011).
- [11] J.-H. Chu, H.-H. Kuo, J. G. Analytis, and I. R. Fisher, *Science* **337**, 710 (2012).
- [12] S. Kasahara, H. J. Shi, K. Hashimoto, S. Tonegawa, Y. Mizukami, T. Shibauchi, K. Sugimoto, T. Fukuda, T. Terashima, A. H. Nevidomskyy, and Y. Matsuda, *Nature (London)* **486**, 382 (2012).
- [13] T. M. Chuang, M. P. Allan, J. Lee, Y. Xie, N. Ni, S. L. Bud'ko, G. S. Boebinger, P. C. Canfield, and J. C. Davis, *Science* **327**, 181 (2010).

- [14] M. P. Allan, T. M. Chuang, F. Masee, Y. Xie, N. Ni, S. L. Bud'ko, G. S. Boebinger, Q. Wang, D. S. Dessau, P. C. Canfield, M. S. Golden, and J. C. Davis, *Nat. Phys.* **9**, 220 (2013).
- [15] S. Liang, A. Moreo, and E. Dagotto, *Phys. Rev. Lett.* **111**, 047004 (2013).
- [16] A. E. Böhmer, P. Burger, F. Hardy, T. Wolf, P. Schweiss, R. Fromknecht, M. Reinecker, W. Schranz, and C. Meingast, *Phys. Rev. Lett.* **112**, 047001 (2014).
- [17] P. Cai, W. Ruan, X. Zhou, C. Ye, A. Wang, X. Chen, D.-H. Lee, and Y. Wang, *Phys. Rev. Lett.* **112**, 127001 (2014).
- [18] R. M. Fernandes, A. V. Chubukov, and J. Schmalian, *Nat. Phys.* **10**, 97 (2014).
- [19] A. Patz, T. Li, S. Ran, R. M. Fernandes, J. Schmalian, S. L. Bud'ko, P. C. Canfield, I. E. Perakis, and J. Wang, *Nat. Commun.* **5**, 3229 (2014).
- [20] S. H. Baek, D. V. Efremov, J. M. Ok, J. S. Kim, J. van den Brink, and B. Buechner, *Nat. Mater.* **14**, 210 (2015).
- [21] J. K. Glasbrenner, I. I. Mazin, H. O. Jeschke, P. J. Hirschfeld, R. M. Fernandes, and R. Valenti, *Nat. Phys.* **11**, 953 (2015).
- [22] A. P. Dioguardi, T. Kissikov, C. H. Lin, K. R. Shirer, M. M. Lawson, H. J. Grafe, J. H. Chu, I. R. Fisher, R. M. Fernandes, and N. J. Curro, *Phys. Rev. Lett.* **116**, 107202 (2016).
- [23] Q. Wang, Y. Shen, B. Pan, Y. Hao, M. Ma, F. Zhou, P. Steffens, K. Schmalzl, T. R. Forrest, M. Abdel-Hafiez, X. Chen, D. A. Chareev, A. N. Vasiliev, P. Bourges, Y. Sidis, H. Cao, and J. Zhao, *Nat. Mater.* **15**, 159 (2016).
- [24] H. C. Xu, X. H. Niu, D. F. Xu, J. Jiang, Q. Yao, Q. Y. Chen, Q. Song, M. Abdel-Hafiez, D. A. Chareev, A. N. Vasiliev, Q. S. Wang, H. L. Wo, J. Zhao, R. Peng, and D. L. Feng, *Phys. Rev. Lett.* **117**, 157003 (2016).
- [25] R. Zhou, L. Y. Xing, X. C. Wang, C. Q. Jin, and G.-q. Zheng, *Phys. Rev. B* **93**, 060502 (2016).
- [26] X. Lu, J. T. Park, R. Zhang, H. Luo, A. H. Nevidomskyy, Q. Si, and P. Dai, *Science* **345**, 657 (2014).
- [27] S. Nandi, M. G. Kim, A. Kreyssig, R. M. Fernandes, D. K. Pratt, A. Thaler, N. Ni, S. L. Bud'ko, P. C. Canfield, J. Schmalian, R. J. McQueeney, and A. I. Goldman, *Phys. Rev. Lett.* **104**, 057006 (2010).
- [28] M. Yi, D. Lu, J.-H. Chu, J. G. Analytis, A. P. Sorini, A. F. Kemper, B. Moritz, S.-K. Mo, R. G. Moore, M. Hashimoto, W.-S. Lee, Z. Hussain, T. P. Devereaux, I. R. Fisher, and Z.-X. Shen, *Proc. Natl. Acad. Sci. USA* **108**, 6878 (2011).
- [29] Y. Gallais, R. M. Fernandes, I. Paul, L. Chauviere, Y. X. Yang, M. A. Measson, M. Cazayous, A. Sacuto, D. Colson, and A. Forget, *Phys. Rev. Lett.* **111**, 267001 (2013).
- [30] C. Mirri, A. Dusza, S. Bastelberger, M. Chinotti, L. Degiorgi, J. H. Chu, H. H. Kuo, and I. R. Fisher, *Phys. Rev. Lett.* **115**, 107001 (2015).
- [31] F. Kretschmar, T. Boehm, U. Karahasanovic, B. Muschler, A. Baum, D. Jost, J. Schmalian, S. Caprara, M. Grilli, C. Di Castro, J. G. Analytis, J. H. Chu, I. R. Fisher, and R. Hackl, *Nat. Phys.* **12**, 560 (2016).
- [32] R. M. Fernandes, L. H. Van Bebber, S. Bhattacharya, P. Chandra, V. Keppens, D. Mandrus, M. A. McGuire, B. C. Sales, A. S. Sefat, and J. Schmalian, *Phys. Rev. Lett.* **105**, 157003 (2010).
- [33] R. Yu and Q. Si, *Phys. Rev. Lett.* **115**, 116401 (2015).
- [34] A. V. Chubukov, M. Khodas, and R. M. Fernandes, *Phys. Rev. X* **6**, 041045 (2016).
- [35] C. C. Lee, W. G. Yin, and W. Ku, *Phys. Rev. Lett.* **103**, 267001 (2009).
- [36] S. Onari and H. Kontani, *Phys. Rev. Lett.* **109**, 137001 (2012).
- [37] Y. Yamakawa, S. Onari, and H. Kontani, *Phys. Rev. X* **6**, 021032 (2016).
- [38] Q. Deng, J. Liu, J. Xing, H. Yang, and H.-H. Wen, *Phys. Rev. B* **91**, 020508 (2015).
- [39] T. Shimojima, K. Ishizaka, Y. Ishida, N. Katayama, K. Ohgushi, T. Kiss, M. Okawa, T. Togashi, X. Y. Wang, C. T. Chen, S. Watanabe, R. Kadota, T. Oguchi, A. Chainani, and S. Shin, *Phys. Rev. Lett.* **104**, 057002 (2010).
- [40] Q. Q. Ge, Z. R. Ye, M. Xu, Y. Zhang, J. Jiang, B. P. Xie, Y. Song, C. L. Zhang, P. Dai, and D. L. Feng, *Phys. Rev. X* **3**, 011020 (2013).
- [41] Y. Zhang, C. He, Z. R. Ye, J. Jiang, F. Chen, M. Xu, Q. Q. Ge, B. P. Xie, J. Wei, M. Aeschlimann, X. Y. Cui, M. Shi, J. P. Hu, and D. L. Feng, *Phys. Rev. B* **85**, 085121 (2012).
- [42] S. V. Carr, C. Zhang, Y. Song, G. Tan, Y. Li, D. L. Abernathy, M. B. Stone, G. E. Granroth, T. G. Perring, and P. Dai, *Phys. Rev. B* **93**, 214506 (2016).
- [43] S. Avci, O. Chmaissem, J. M. Allred, S. Rosenkranz, I. Eremin, A. V. Chubukov, D. E. Bugaris, D. Y. Chung, M. G. Kanatzidis, J. P. Castellan, J. A. Schlueter, H. Claus, D. D. Khalyavin, P. Manuel, A. Daoud-Aladine, and R. Osborn, *Nat. Commun.* **5**, 3845 (2014).
- [44] C. Giannetti, M. Capone, D. Fausti, M. Fabrizio, F. Parmigiani, and D. Mihailovic, *Adv. Phys.* **65**, 58 (2016).
- [45] E. E. Chia, D. Talbayev, J. X. Zhu, H. Q. Yuan, T. Park, J. D. Thompson, C. Panagopoulos, G. F. Chen, J. L. Luo, N. L. Wang, and A. J. Taylor, *Phys. Rev. Lett.* **104**, 027003 (2010).
- [46] T. Mertelj, V. V. Kabanov, C. Gadermaier, N. D. Zhigadlo, S. Katrych, J. Karpinski, and D. Mihailovic, *Phys. Rev. Lett.* **102**, 117002 (2009).
- [47] W. Li, C. Zhang, S. Liu, X. Ding, X. Wu, X. Wang, H.-H. Wen, and M. Xiao, *Phys. Rev. B* **89**, 134515 (2014).
- [48] S. Dal Conte, C. Giannetti, G. Coslovich, F. Cilento, D. Bossini, T. Abebaw, F. Banfi, G. Ferrini, H. Eisaki, M. Greven, A. Damascelli, D. van der Marel, and F. Parmigiani, *Science* **335**, 1600 (2012).
- [49] S. Dal Conte, L. Vidmar, D. Golez, M. Mierzejewski, G. Soavi, S. Peli, F. Banfi, G. Ferrini, R. Comin, B. M. Ludbrook, L. Chauviere, N. D. Zhigadlo, H. Eisaki, M. Greven, S. Lupi, A. Damascelli, D. Brida, M. Capone, J. Bonca, G. Cerullo, and C. Giannetti, *Nat. Phys.* **11**, 421 (2015).
- [50] J. P. Hinton, J. D. Koralek, G. Yu, E. M. Motoyama, Y. M. Lu, A. Vishwanath, M. Greven, and J. Orenstein, *Phys. Rev. Lett.* **110**, 217002 (2013).
- [51] D. H. Torchinsky, G. F. Chen, J. L. Luo, N. L. Wang, and N. Gedik, *Phys. Rev. Lett.* **105**, 027005 (2010).
- [52] Y. C. Wen, K. J. Wang, H. H. Chang, J. Y. Luo, C. C. Shen, H. L. Liu, C. K. Sun, M. J. Wang, and M. K. Wu, *Phys. Rev. Lett.* **108**, 267002 (2012).
- [53] G. Coslovich, C. Giannetti, F. Cilento, S. Dal Conte, T. Abebaw, D. Bossini, G. Ferrini, H. Eisaki, M. Greven, A. Damascelli, and F. Parmigiani, *Phys. Rev. Lett.* **110**, 107003 (2013).
- [54] C. W. Luo, I. H. Wu, P. C. Cheng, J. Y. Lin, K. H. Wu, T. M. Uen, J. Y. Juang, T. Kobayashi, D. A. Chareev, O. S. Volkova, and A. N. Vasiliev, *Phys. Rev. Lett.* **108**, 257006 (2012).
- [55] J. Demsar, J. L. Sarrao, and A. J. Taylor, *J. Phys.: Condens. Matter* **18**, R281 (2006).

- [56] L. Stojchevska, T. Mertelj, J.-H. Chu, I. R. Fisher, and D. Mihailovic, *Phys. Rev. B* **86**, 024519 (2012).
- [57] C.-W. Luo, P. C. Cheng, S.-H. Wang, J.-C. Chiang, J.-Y. Lin, K.-H. Wu, J.-Y. Juang, D. A. Chareev, O. S. Volkova, and A. N. Vasiliev, *npj Quantum Mater.* **2**, 32 (2017).
- [58] Q. Deng, J. Xing, J. Liu, H. Yang, and H.-H. Wen, *Phys. Rev. B* **92**, 014510 (2015).
- [59] W. Z. Hu, G. Li, P. Zheng, G. F. Chen, J. L. Luo, and N. L. Wang, *Phys. Rev. B* **80**, 100507 (2009).
- [60] See Supplemental Material at <http://link.aps.org/supplemental/10.1103/PhysRevB.97.020505> for fluence dependence of transient reflectivity, polarization configuration, static reflectivity, long scale time-resolved kinetics, different samples' experiments, pressure effect, description of third-order nonlinear optical response and polarization-dependent electronic transitions.
- [61] J. D. Wright, T. Lancaster, I. Franke, A. J. Steele, J. S. Möller, M. J. Pitcher, A. J. Corkett, D. R. Parker, D. G. Free, F. L. Pratt, P. J. Baker, S. J. Clarke, and S. J. Blundell, *Phys. Rev. B* **85**, 054503 (2012).
- [62] D. H. Torchinsky, J. W. McIver, D. Hsieh, G. F. Chen, J. L. Luo, N. L. Wang, and N. Gedik, *Phys. Rev. B* **84**, 104518 (2011).
- [63] R. W. Boyd, *Nonlinear Optics* (Elsevier, Amsterdam, 2010).
- [64] Y. Toda, F. Kawanokami, T. Kurosawa, M. Oda, I. Madan, T. Mertelj, V. V. Kabanov, and D. Mihailovic, *Phys. Rev. B* **90**, 094513 (2014).
- [65] H. Kontani, T. Saito, and S. Onari, *Phys. Rev. B* **84**, 024528 (2011).
- [66] C. He, Y. Zhang, X. F. Wang, J. Jiang, F. Chen, L. X. Yang, Z. R. Ye, F. Wu, M. Arita, K. Shimada, H. Namatame, M. Taniguchi, X. H. Chen, B. P. Xie, and D. L. Feng, *J. Phys. Chem. Solids* **72**, 479 (2011).
- [67] M. Yi, D. H. Lu, R. G. Moore, K. Kihou, C. H. Lee, A. Iyo, H. Eisaki, T. Yoshida, A. Fujimori, and Z. X. Shen, *New J. Phys.* **14**, 073019 (2012).
- [68] A. V. Boris, N. N. Kovaleva, S. S. A. Seo, J. S. Kim, P. Popovich, Y. Matiks, R. K. Kremer, and B. Keimer, *Phys. Rev. Lett.* **102**, 027001 (2009).
- [69] A. Charnukha, P. Popovich, Y. Matiks, D. L. Sun, C. T. Lin, A. N. Yaresko, B. Keimer, and A. V. Boris, *Nat. Commun.* **2**, 219 (2011).
- [70] M. Fox, *Optical Properties of Solids* (Oxford University Press, Oxford, U.K., 2001).
- [71] S. K. Nair, X. Zou, E. E. M. Chia, J.-X. Zhu, C. Panagopoulos, S. Ishida, and S. Uchida, *Phys. Rev. B* **82**, 212503 (2010).
- [72] P. Cai, X. Zhou, W. Ruan, A. Wang, X. Chen, D.-H. Lee, and Y. Wang, *Nat. Commun.* **4**, 1596 (2013).
- [73] A. Martinelli, A. Palenzona, M. Putti, and C. Ferdeghini, *Phys. Rev. B* **85**, 224534 (2012).
- [74] P. Kusar, V. V. Kabanov, J. Demsar, T. Mertelj, S. Sugai, and D. Mihailovic, *Phys. Rev. Lett.* **101**, 227001 (2008).
- [75] J. Wu, A. T. Bollinger, X. He, and I. Bozovic, *Nature (London)* **547**, 432 (2017).
- [76] S. Yonezawa, K. Tajiri, S. Nakata, Y. Nagai, Z. Wang, K. Segawa, Y. Ando, and Y. Maeno, *Nat. Phys.* **13**, 123 (2017).
- [77] J. W. Harter, Z. Y. Zhao, J. Q. Yan, D. G. Mandrus, and D. Hsieh, *Science* **356**, 295 (2017).
- [78] F. Ronning, T. Helm, K. R. S. Hirer, M. D. Bachmann, L. Balicas, M. K. Chan, B. J. Ramshaw, R. D. McDonald, F. F. Balakirev, M. Jaime, E. D. Bauer, and P. J. W. Moll, *Nature (London)* **548**, 313 (2017).
- [79] L. Ma, J. Dai, P. S. Wang, X. R. Lu, Y. Song, C. L. Zhang, G. T. Tan, P. C. Dai, D. Hu, S. L. Li, B. Normand, and W. Q. Yu, *Phys. Rev. B* **90**, 144502 (2014).